Accepted: 14 March 2018

DOI: 10.1111/epi.14070

FULL-LENGTH ORIGINAL RESEARCH

Epilepsia®

Nonconvulsive status epilepticus in rats leads to brain pathology

Una Avdic[1,2] | Matilda Ahl[1,2] | Deepti Chugh[1,2] | Idrish Ali[1,2] | Karthik Chary[3] | Alejandra Sierra[3] | Christine T. Ekdahl[1,2]

[1]Division of Clinical Neurophysiology, Inflammation and Stem Cell Therapy Group, Lund University, Lund, Sweden

[2]Department of Clinical Sciences, Epilepsy Center, Lund University, Lund, Sweden

[3]Biomedical Imaging Unit, A. I. Virtanen Institute for Molecular Sciences, University of Eastern Finland, Kuopio, Finland

Correspondence
Christine T. Ekdahl, Division of Clinical Neurophysiology, Inflammation and Stem Cell Therapy Group, Lund University, Lund, Sweden.
Email: christine.ekdahl_clementson@med.lu.se

Funding information
European Union's Seventh Framework Program, Grant/Award Number: 602102; Swedish Research Council; Crafoord Foundation; Academy of Finland, Grant/Award Number: 275453

Summary

Objective: Status epilepticus (SE) is an abnormally prolonged epileptic seizure that if associated with convulsive motor symptoms is potentially life threatening for a patient. However, 20%-40% of patients with SE lack convulsive events and instead present with more subtle semiology such as altered consciousness and less motor activity. Today, there is no general consensus regarding to what extent nonconvulsive SE (NCSE) is harmful to the brain, which adds uncertainty to stringent treatment regimes.

Methods: Here, we evaluated brain pathology in an experimental rat and mouse model of complex partial NCSE originating in the temporal lobes with Western blot analysis, immunohistochemistry, and ex vivo diffusion tensor imaging (DTI). The NCSE was induced by electrical stimulation with intrahippocampal electrodes and terminated with pentobarbital anesthesia. Video-electroencephalographic recordings were performed throughout the experiment.

Results: DTI of mice 7 weeks post-NCSE showed no robust long-lasting changes in fractional anisotropy within the hippocampal epileptic focus. Instead, we found pathophysiological changes developing over time when measuring protein levels and cell counts in extracted brain tissue. At 6 and 24 hours post-NCSE in rats, few changes were observed within the hippocampus and cortical or subcortical structures in Western blot analyses of key components of the cellular immune response and synaptic protein expression, while neurodegeneration had started. However, 1 week post-NCSE, both excitatory and inhibitory synaptic protein levels were decreased in hippocampus, concomitant with an excessive microglial and astrocytic activation. At 4 weeks, a continuous immune response in the hippocampus was accompanied with neuronal loss. Levels of the excitatory synaptic adhesion molecule N-cadherin were decreased specifically in rats that developed unprovoked spontaneous seizures (epileptogenesis) within 1 month following NCSE, compared to rats only exhibiting acute symptomatic seizures within 1 week post-NCSE.

Significance: These findings provide evidence for a significant brain pathology following NCSE in an experimental rodent model.

KEYWORDS
diffusion tensor imaging, inflammation, N-cadherin, nonconvulsive status epilepticus, synaptic proteins

1 | INTRODUCTION

Status epilepticus (SE) is a severe neurological condition characterized by prolonged seizure activity that may be fatal if not interrupted. It typically manifests with convulsive movements, but 20%-40% of SE cases present a more heterogeneous semiology referred to as nonconvulsive SE (NCSE).[1–3] Common clinical manifestations of NCSE are altered consciousness, automatisms, and subtle motor activity such as lip smacking or stereotypic orofacial/hand/arm movements, and they often involve the frontotemporal brain regions.[1,4] NCSE can be difficult to diagnose, especially in comatose patients.

Convulsive SE for >30 minutes, regardless of the triggering factor, can be fatal and leads to substantial neuronal death in the brain. To what extent NCSE, which may either be cryptogenic or arise due to other brain insults, could injure the brain is not clear. So far, the general clinical prediction of NCSE is that it may not give rise to long-lasting changes in the brain. Magnetic resonance imaging (MRI), single photon emission computed tomography, and diffusion tensor imaging (DTI) of patients with ongoing NCSE have shown perictal abnormalities including regional hyperperfusion and reduced diffusion, but on follow-up MRI most patients show complete resolution.[5,6] Consequently, when considering aggressive anesthetic therapy to terminate drug-resistant NCSE the clinical knowledge of possible brain injuries due to the NCSE per se is lacking and the treatment is mostly dependent on the underlying disease.[1]

A number of experimental animal models have been utilized to study disease mechanisms of SE, with the chemical pilocarpine/kainic acid models being the most frequently used.[7–10] Electrical stimulation with intracranial electrodes to generate an epileptic focus is also a well-established model.[11] Primarily, these models are used to induce secondary generalized and convulsive seizures. There is a lack of extensive experimental studies defining significant NCSE-induced brain pathology.

The pathophysiology that follows upon prolonged convulsive seizures involves a disruption of the common balance between excitatory and inhibitory neuronal pathways, which are normally regulated by a number of proteins within the neuronal synapses, including adhesion molecules and scaffolding proteins such as neuroligins and cadherins.[12,13] The latter are important for spine shape, synaptic establishment, transmission, and strength, and thus network excitability.[13,14] Synaptic dysregulation is closely related to both neuronal death and glial activation.[15,16] How the levels of synaptic proteins may change in the brain following NCSE is hardly known.

In the current study, we utilize a protocol for NCSE originating from the temporal lobes, induced by electrical stimulation.[11,17] We describe semiology and electroencephalographic (EEG) pattern during NCSE, the degree of acute symptomatic and spontaneous seizures, and interictal activity (IA) post-NCSE. We investigate whether DTI detects robust long-lasting structural changes in the brain and whether neuronal loss, immune reaction, and alterations in synaptic proteins may be detectable in brain tissue at several time points post-NCSE.

Key Points

- NCSE leads to brain pathology
- NCSE leads to inflammation in the brain and a disruption in synaptic proteins important for maintaining the excitatory/inhibitory balance
- This experimental complex partial NCSE model shares similarities in EEG patterns/semiology with clinical presentations of NCSE
- Rats with NCSE display both acute symptomatic seizures and spontaneous recurrent seizures
- Rats with NCSE and spontaneous seizures have decreased levels of the excitatory adhesion molecule N-cadherin in the epileptic focus

2 | MATERIALS AND METHODS

2.1 | Animals

Adult male Sprague-Dawley rats (n = 85) weighing 200-250 g and male C57/BL mice (n = 6) were procured from Charles River (Sulzfeld, Germany) and housed with a 12-hour light/dark cycle and ad libitum food and water. Experimental procedures followed guidelines set by the Malmö-Lund Ethical Committee in Sweden for use and care of laboratory animals. Every effort was made to limit the number of animals used. ARRIVE (Animal Research: Reporting of In Vivo Experiments) guidelines were considered when planning the experiments. Animals were randomly divided into the different experimental groups and analyzed by researchers who were blind to the treatment condition. Male rats and mice were used to compare data with a previous similar epilepsy model.[17,18]

2.2 | Group assignment

Rats were divided into 4 survival groups following electrically induced NCSE and corresponding electrode-implanted nonstimulated controls (Ctrl): 6 hours (NCSE, n = 7; Ctrl, n = 8), 24 hours (NCSE, n = 11; Ctrl, n = 11), 1 week (NCSE, n = 6; Ctrl, n = 6), 4 weeks (NCSE, n = 16; Ctrl, n = 12). At 4 weeks, a subset of rats had developed spontaneous recurrent seizures (n = 12) whereas others only

displayed acute symptomatic seizures during the 1 week following NCSE (n = 4). Immunohistochemical analyses were performed on a separate group of rats at 4 weeks following NCSE. These animals also had an implanted anterior intraventricular cannula, ipsilateral to the electrode (NCSE, n = 6; Ctrl, n = 9) and serve as Ctrl in a separate project (Avdic et al, unpublished observations). Six mice (Ctrl, n = 3; NCSE, n = 3) were used for DTI.

2.3 | Electrically induced NCSE

Animals were anesthetized with 1.5%-2% isoflurane and implanted with a bipolar insulated stainless steel electrode (Plastics One, Roanoke, VA, USA) into the right ventral CA1/CA3 region of the hippocampus (HPC; coordinates in rats: 4.8 mm posterior, 5.2 mm lateral from bregma, and 6.3 mm ventral from dura, tooth bar = −3.0 mm; coordinates mice: 2.9 mm posterior, 3.0 mm lateral from bregma, and 3.0 mm ventral from dura, tooth bar = −3.0 mm) for stimulation and recording. A unipolar electrode was placed between the skull and adjacent muscle to serve as ground electrode. Following 1 week of recovery after surgery, animals were subjected to 1 hour of electrical stimulation according to a previously described protocol.[17] Only animals that after 1 hour of stimulation displayed self-sustained ictal EEG activity for 2 hours with mainly complex partial seizure semiology, including immobility, stereotypic hyperactive explorative behavior without reacting to sudden sounds such as clapping, orofacial twitches, head nodding, drooling, and/or unilateral forelimb clonus, were included. Behavioral symptoms and ictal EEG activity were interrupted after 2 hours of self-sustained NCSE by administration of pentobarbital (65 mg/kg, intraperitoneal injection; Figure 1).

2.4 | EEG evaluations

Animals were continuously video-EEG–monitored (24 h/d) throughout the experimental procedure (Powerlab and Labchart v8.1.1; AD Instruments, Dunedin, New Zealand; sampling frequency = 1000 Hz). The EEG from intrahippocampal electrodes was visually evaluated and quantified in terms of EEG patterns during NCSE, number of spontaneous and acute symptomatic seizures, and IA. Seizures (both acute symptomatic, which occur within 1 week after NCSE, and spontaneous, starting day 8 post-NCSE)[19,20] were defined as epileptiform EEG activity lasting ≥10 seconds with an evolving pattern, typically consisting of initial high-frequency low-amplitude activity that over time increases in amplitude and decreases in frequency as a spike–slow-wave pattern. Seizure frequency was quantified manually, and the total time animals exhibited seizure activity was divided into days 0-7 and 8-28 post-NCSE. IA was graded according to a 0-5 scale (0 = none, 1 = <10 spikes/h, 2 = approximately 50 spikes/h, 3 = approximately 80 spikes/h, 4 = approximately 100 spikes/h, and 5 = >150 spikes/h).

2.5 | Tissue preparation

For DTI, mice were anesthetized and transcardially perfused with 0.9% saline for 3 minutes, followed by 4% paraformaldehyde for 15 minutes, before decapitation. Intact heads were postfixed overnight and washed with 0.9% saline for >12 hours. Prior to imaging, heads were placed in perfluoro polyether (Galden HS240; Vacuumservice Oy, Helsinki, Finland) to prevent drying and suppress background signal.

For biochemical analyses, rats were decapitated and brains were immediately removed, divided into ipsilateral and contralateral hemispheres related to electrode implantation, further dissected into HPC, cortex, and subcortex, frozen on dry ice, and stored at −80°C. Homogenization and determination of protein concentration were performed as previously described.[21]

Details on immunohistochemical processing, Fluoro-Jade (FJ) and hematoxylin-eosin (H&E) stainings and cell counts can be found in the supporting information.

2.6 | Diffusion tensor imaging acquisition, data processing, and data analysis

Mouse brains were imaged ex vivo in a 9.4-T magnet (Oxford Instruments, Abingdon, UK). Details on acquisition parameters are provided in the supporting information. A voxelwise fit of the diffusion tensor model was performed to generate fractional anisotropy (FA) maps. FA maps were analyzed using in-house built-in MATLAB software (AEDES; http://aedes.uef.fi). In FA maps, 3 adjacent images at 2.92 mm posterior from bregma were analyzed. Two regions of interest (ROIs) within the epileptic focus were manually marked; dorsal molecular layer (dML) of the supragranular blade of the dentate gyrus in HPC, with no visually observed blurriness, and the ventral CA3 region with visual blurriness (Figure 1C).

2.7 | Western blot analysis

Western blot analysis was performed as previously described.[22] For a detailed list of primary antibodies (Abs) see Table S1. Secondary Abs used were either horseradish peroxidase–conjugated antimouse (1:5000), antigoat (1:5000), or antirabbit (1:5000; Sigma, St. Louis, MO, USA). Band intensities were quantified using ImageJ software. Relative protein expression was compared to the control levels and normalized by expression of internal control β-actin or glyceraldehyde-3-phosphate dehydrogenase levels.

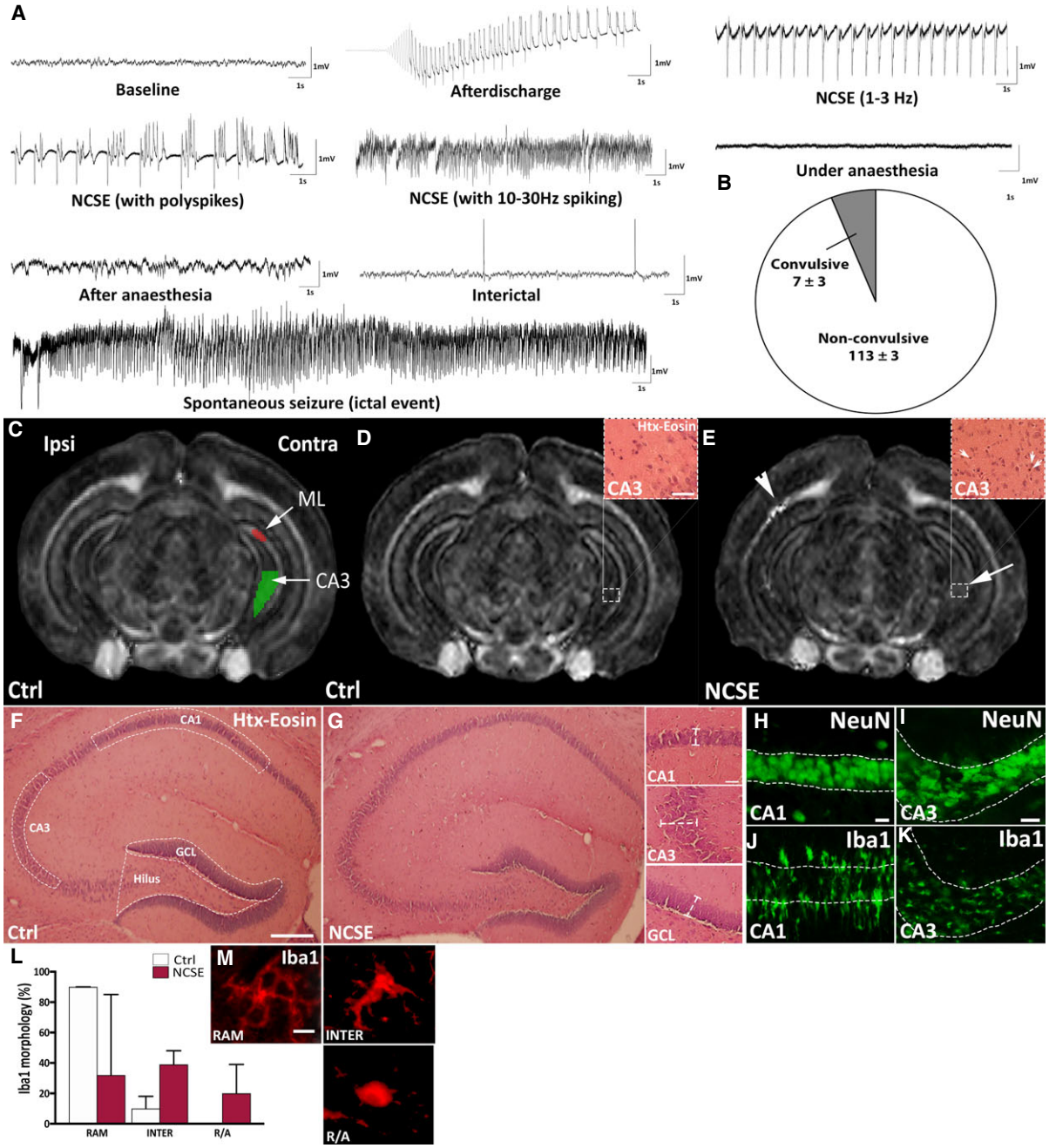

FIGURE 1 Intrahippocampal electroencephalogram recordings, diffusion tensor imaging (DTI), and histopathology of rodent brain following nonconvulsive status epilepticus (NCSE). A, Representative background activity before stimulation (baseline), epileptiform afterdischarge during 1 hour of stimulation, epileptiform activity with varying frequency during 2 hours of self-sustained complex partial NCSE, and background activity during and after waking up from anesthesia when NCSE was terminated with pentobarbital injection, an example of a spontaneous seizure with evolving pattern, and interictal epileptiform activity. B, Pie chart showing the mean percentage of time exhibiting nonconvulsive or convulsive seizure semiology during 2 hours of NCSE. C-E, Representative DTI images of nonstimulated control mice (Ctrl) and 7 weeks post-NCSE. C, Regions of interest for fractional anisotropy analysis in CA3 (green) and dorsal molecular layer (ML) of dentate gyrus (red) contralateral to electrode implantation. Arrow in E marks occasional structural disruption in ventral CA3 of NCSE mice and arrowhead points at the tissue damage due to the electrode. Insets in D and E show higher-magnification of hematoxylin-eosin (Htx-Eosin) staining in CA3. Note the clustering of small cell nuclei (arrows) in E. F, G, Representative images of hippocampus in hematoxylin-eosin staining from Ctrl (F) and NCSE (G) and panel of high-magnification of CA1, CA3, and granular cell layer (GCL). Dotted lines mark area and examples of width for measurements of layer thickness. H, I, and J, K NeuN- and Iba1-positive cells included in stereological counting in CA1 and CA3 7 weeks post-NCSE, respectively. L, M, Quantification of relative percentage and microphotographs of Iba1-positive cells with different morphologies, including ramified (RAM), intermediate (INTER), and round/amoeboid (R/A). Scalebar in D represents 25 μm, F represents 500 μm, in H represents 10 μm in H and J, in I represents 10 μm in I and K, and in M represents 10 μm

2.8 | Statistical analysis

Statistical analyses were performed with unpaired and paired Student *t* tests when comparing 2 groups, using GraphPad (La Jolla, CA, USA) Prism software. Interictal analysis, grading of FJ^+ cells, and stereology of Iba1 and NeuN in mice (n = 3) were analyzed with nonparametric Mann-Whitney test, the latter due to nonnormal distribution of numbers. Data are presented as mean ± standard error of mean or median ± range, unless otherwise stated. Differences were considered statistically significant at $P \leq .05$.

3 | RESULTS

3.1 | EEG and semiology of NCSE and the development of spontaneous seizures in rats

After 1 hour of electrical stimulation of the right HPC, all included rats exhibited self-sustained seizure activity for 2 hours, confirmed by continuous epileptiform EEG activity, and nonconvulsive seizure semiology (94% of the time, <6% of the time convulsive semiology with bilateral fore-/hindlimb clonus; Figure 1A,B). Intraperitoneal anesthesia was used to interrupt ictal activity. The EEG patterns during NCSE included the most common pattern found in clinical practice: periodic rhythmic discharges of low frequencies (1-3 Hz), with or without polyspike formations, mixed with periods of evolving buildup of a rhythmic high-frequency pattern (Figure 1A).[3,23,24]

Following NCSE, in total 88% of all rats experienced acute symptomatic seizures (100% in 6 hours, 67% in 24 hours, 83% in 1 week, and 93% in 4 weeks group). Of the 93% in the 4-week group, 29% exhibited only acute symptomatic, whereas 71% developed both acute symptomatic and spontaneous seizures. A subset of rats in the 4-week group (35%) regained their NCSE within 5 hours after anesthesia, of which 30% exhibited only acute symptomatic, whereas 60% also developed spontaneous seizures. The mean duration of the regained NCSE measured 338 ± 72.7 minutes, and the vast majority self-terminated. The rest received a second anesthesia and were terminated permanently. The mean total duration of all EEG-verified spontaneous seizures per rat during weeks 2-4 in the 4-week survival group measured 32 ± 12 minutes, whereas their total load of acute symptomatic seizures during the first week post-NCSE was 10.2 ± 2.6 minutes. Rats with only acute symptomatic seizures exhibited an ictal load of 3.6 ± 1.6 minutes, which did not differ significantly from rats with spontaneous epileptic seizures. The spontaneous seizures consisted of both nonconvulsive (majority) and convulsive semiology.

Interictal grading (amount of interictal epileptiform activity) of the EEG from the 4-week survival group showed no differences between rats with spontaneous and only acute symptomatic seizures during the first week post-NCSE (2.6 ± 0.30 vs 2.0 ± 0.2) or during weeks 2-4 (2.4 ± 0.3 vs 2.0 ± 0.3, where grade 2 was defined as approximately 50 spikes/h). The NCSE rats experienced no weight loss compared to Ctrl at 4 weeks post-NCSE (Ctrl 426.4 ± 14.4 g vs NCSE 421.3 ± 11.4 g).

3.2 | DTI analysis of mouse brain 7 weeks after NCSE

DTI is an MRI-based imaging technique that detects water diffusion and enables measurement of microstructural alterations in the tissue. We have previously demonstrated epileptic insults after kainic acid–induced convulsive SE.[25] Visual assessment on DTI maps of the epileptic focus in the temporal lobe after NCSE (Figure 1C-E) indicated a disrupted integrity of the ventral HPC layers contralateral to the electrode-implanted side (Figure 1D, arrow) in a small group of mice 7 weeks post-NCSE. However, quantitative analysis of FA in the contralateral ventral CA3 and dML showed no significant differences compared to Ctrl (CA3: Ctrl 0.19 ± 0.02 vs NCSE 0.22 ± 0.01; dML: Ctrl 0.33 ± 0.06 vs NCSE 0.35 ± 0.02). When evaluating the cytoarchitecture of the contralateral HPC with H&E staining, no differences in gray layer thickness were observed, suggesting that no robust cell layer dispersion had occurred (Figure 1F,G, Table S2). The density of $NeuN^+$ and $Iba1^+$ cells was not different (Figure 1H-K, Table S2). Due to high variation in numbers of $Iba1^+$ cells in CA1/CA3 of the NCSE group, we also analyzed the morphology of $Iba1^+$ cells in these regions and found a difference in the percentage of phenotypes, where the NCSE group had relatively less ramified/surveying compared to more activated intermediate/round/amoeboid $Iba1^+$ cells (Figure 1L,M). Due to electrode disturbances, ROI analyses were not performed for ipsilateral HPC. The NCSE mice exhibited similar EEG patterns and semiology during NCSE as rats, with 98.5% nonconvulsive semiology and continuous epileptiform EEG activity during 2 hours. No continuous video-EEG was performed during the 7 weeks post-NCSE; hence, the mice could not be further divided into acute symptomatic or epileptogenic animals.

3.3 | Neuronal loss and glial activation within the epileptic focus following NCSE in rats

Because our cohort of DTI-imaged mice supported the clinical experiences of the difficulties in detecting robust long-lasting structural changes due to NCSE, we continued to evaluate possible biochemical tissue alterations, such as protein levels representative of neuronal loss and immune reactions. The amounts of neurons (NeuN), microglia

(Iba1), and astrocytes (glial fibrillary acidic protein [GFAP], S100β) were analyzed in cortical, subcortical, and HPC tissue 6 and 24 hours, and 1 and 4 weeks post-NCSE (Figure 2A-E). Due to possible local damage inflicted by the intraparenchymal electrodes, ipsilateral HPC and contralateral HPC were analyzed separately. At 6 hours post-NCSE, total protein levels of NeuN (Figure 2A), Iba1, GFAP, and S100β remained unchanged in contralateral HPC (Table S4). No changes were detected in ipsilateral HPC, cortex, and subcortex, except for an increase in GFAP in subcortical structures (Table 1). At 24 hours following NCSE, a common time point when the pathophysiology starts to manifest after convulsive seizures,[26] we detected region-specific FJ^+ labeling particularly in CA1 and CA3 (Figure 2B), whereas there was no significant difference in the dentate hilus (Ctrl 3.1 ± 0.8 vs NCSE 7.9 ± 3.4 cells/section). Despite ongoing neurodegeneration, analyses showed no alterations in NeuN protein levels in ipsilateral and contralateral HPC tissue (Figure 2A, Table 1). Similarly, Iba1 and GFAP levels remained unchanged whereas S100β increased slightly in contralateral HPC (Table S4). No changes were detected in ipsilateral HPC (Table 1). At 1 week post-NCSE, more prominent changes started to occur. Both Iba1 and GFAP levels were increased in ipsilateral and contralateral HPC at this time point, whereas NeuN and S100β (Ctrl 100 ± 14.2 vs NCSE 131.3 ± 5.8) levels remained unaltered (Figure 2A,D,E). No changes were observed in cortical and subcortical tissue (Table 1). At 4 weeks post-NCSE, the GFAP and Iba1 response persisted in contralateral HPC as well as GFAP and S100β on the ipsilateral side (Figure 2D,E, Table 1). S100β levels remained unchanged in the contralateral HPC (Ctrl 100 ± 9.4 vs NCSE 94.3 ± 2.6). Interestingly, NeuN levels were now decreased in the contralateral HPC (Figure 2A), accompanied by a decrease in $NeuN^+$ cell density in CA1 (Figure 2C). No changes were detected in CA3, granular cell layer, or dentate hilus (Table S3). In addition, $Iba1^+$ cell density was increased in CA1 (Figure 2D) and not in other HPC subregions (Table S3). No signs of layer dispersion and differences in thickness were observed on H&E staining in the HPC (Figure 2C, Table S3). At this time point, increased Iba1 and decreased NeuN levels were observed in ipsilateral compared to contralateral HPC tissue from Ctrl (120.4 ± 14.0 vs 47.8 ± 7.2 and 77.3 ± 12.4 vs 172.3 ± 7.1, respectively), probably due to electrode-induced damage. This confounder makes analyses of ipsilateral HPC difficult to interpret and may hide possible changes in NCSE rats. The reduced levels of NeuN in contralateral HPC were accompanied by a decrease in parvalbumin (PV) and an increase in neuropeptide Y (NPY) expression (PV, Ctrl 100 ± 9.0 vs NCSE 74.8 ± 3.9; NPY: Ctrl 100 ± 24.9 vs NCSE 255.2 ± 36.5 respectively), 2 proteins abundant in inhibitory neurons within the HPC.[27] In accordance with earlier time points, no alterations were observed in cortical tissue whereas GFAP and S100β levels were increased in subcortex (Table 1).

3.4 | Decreased levels of synaptic proteins following NCSE

To determine how NCSE may lead to alterations of the excitatory/inhibitory balance, we decided to evaluate synaptic proteins related to both excitatory (PSD-95, NL-1, N-cadherin) and inhibitory postsynaptic structures (gephyrin, NL-2, neurofascin [NF]), as well as presynaptic vesicle-related proteins (synapsin I and synapsin II). At 6 and 24 hours after NCSE, none of the synaptic proteins was altered in either ipsi-/contralateral HPC, cortex, or subcortex, except for an increase at 6 hours of NL1,[12] an excitatory adhesion molecule, within ipsilateral HPC and a reduction of the excitatory scaffolding protein PSD-95,[21,28] a mediator of glutamatergic excitatory synapse clustering in cortical tissue (Tables 1 and 2).

At 1week post-NCSE, when rats had exhibited acute symptomatic seizures, levels of PSD-95 and NL-1[29] were decreased in the contralateral HPC, whereas the excitatory synapse-associated adhesion molecule N-cadherin was unaltered. At the inhibitory synapses, the postsynaptic scaffolding protein gephyrin was reduced, but not accompanied by a change in the adhesion molecule NL-2 or NF.[12,21] Synapsin II was reduced, whereas synapsin I levels remained unaltered (Figure 3). In the ipsilateral HPC, both NL-2 and synapsin II were reduced (Table 1). Again, protein levels did not change in the cortex and subcortex, except for a small decrease in N-cadherin[21] levels in the subcortex (Table 1). At 4 weeks post-NCSE, no changes in synaptic protein levels were detected in the contralateral or ipsilateral HPC compared to Ctrl. Similarly, no alterations were detected in the cortex and subcortex, apart from a minor increase in synapsin II in the cortex (Tables 1 and 2).

3.5 | Development of unprovoked spontaneous seizures following NCSE correlates partly to neuronal loss and glial activation

To assess to what extent the development of spontaneous seizures after NCSE (ie, epileptogenesis) correlates to the neuronal loss, glial activation, and changes in synaptic protein levels, we subdivided the 4-week NCSE rats into 2 groups: rats with only acute symptomatic seizures within 1week (NCSE+AS) and rats with additional spontaneous seizures during 2-4 weeks post-NCSE (NCSE+SS). The

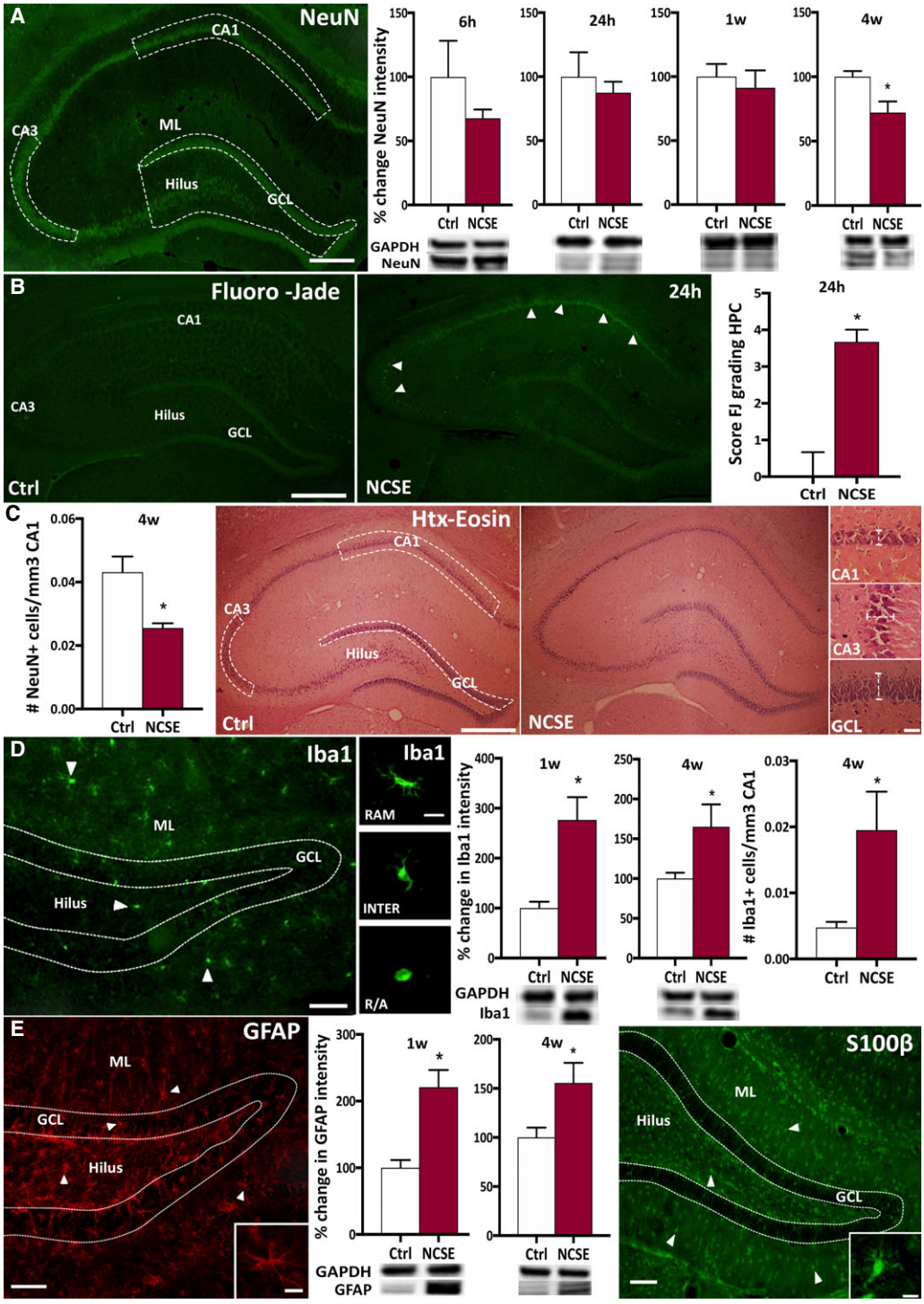

FIGURE 2 Neuronal loss and glial activation following nonconvulsive status epilepticus (NCSE). Representative images show immunohistochemical stainings, immunoblots, and quantification of NeuN (46 kDa; A), Fluoro-Jade (FJ; B), NeuN and hematoxylin-eosin (Htx-Eosin; C), Iba1 (17 kDa; D), and glial fibrillary acidic protein (GFAP; 55 kDa) and S100β (11 kDa; E) at different time points following NCSE relative to controls (Ctrl). Immunoblots are normalized to glyceraldehyde-3-phosphate dehydrogenase (GAPDH; 37 kDa). Data are presented as mean ± standard error of mean, n = 8 Ctrl and n = 7 NCSE for 6-hour group, n = 8 Ctrl and n = 6 NCSE for immunoblots, and n = 5 Ctrl and n = 3 NCSE for Fluoro-Jade staining in 24-hour group, n = 6 Ctrl and n = 6 NCSE for 1-week group, and n = 13 Ctrl and n = 16 NCSE for immunoblots and n = 9 Ctrl and n = 6 NCSE for immunohistochemical analysis of NeuN in 4-week group. *$P \leq .05$, unpaired t test. ML = molecular layer, GCL = granule cell layer within contralateral hippocampus (HPC). Higher magnification in D represents RAM = ramified, INTER = intermediate, and R/A = round/amoeboid Iba1 morphology. Arrowheads in B, D, and E point toward cells positive for Fluoro-Jade, Iba1, and GFAP and S100β, respectively. Scale bars represent 500 μm in A-C, 100 μm in D-E, 50 μm in the higher magnification panel in C, and 10 μm in insets in D and E

TABLE 1 Quantification of immunoblots of neuronal, microglial, and astrocytic markers and excitatory and inhibitory synaptic proteins in ipsilateral hippocampus, cortex, and subcortex at 6 hours, 24 hours, 1 week, and 4 weeks post-NCSE

	Ipsilateral HPC		Cortex		Subcortex	
	Ctrl	**NCSE**	**Ctrl**	**NCSE**	**Ctrl**	**NCSE**
Neurons and glial cells						
6 h						
NeuN	100 ± 28.9	140.9 ± 25.8	100 ± 18.9	96.2 ± 28.5	100 ± 12.0	142.8 ± 43.8
Iba1	100 ± 167.0	117.1 ± 21.7	100 ± 4.6	84.8 ± 5.5	100 ± 13.2	143.2 ± 31.0
GFAP	100 ± 14.9	93.9 ± 17.2	100 ± 5.9	86.1 ± 8.4	**100 ± 41.0**	**462.7 ± 120.5**[a]
S100β	100 ± 5.6	113.6 ± 9.5	100 ± 29.8	71.9 ± 22.7	100 ± 11.4	117.8 ± 25.8
24 h						
NeuN	100 ± 13.9	76.8 ± 18.0	100 ± 24.1	137.7 ± 38.9	100 ± 52.9	38.5 ± 8.3
Iba1	100 ± 6.3	109.4 ± 17.4	100 ± 11.7	85.6 ± 18.6	100 ± 11.6	187.8 ± 57.1
GFAP	100 ± 2.6	107.1 ± 22.9	100 ± 15.9	137.2 ± 26.1	100 ± 9.2	168.3 ± 54.6
S100β	100 ± 5.5	97.5 ± 2.4	100 ± 15.6	76.4 ± 4.3	100 ± 15.3	102.1 ± 23.6
1 wk						
NeuN	100 ± 11.8	121.4 ± 10.7	100 ± 17.8	124.3 ± 18.3	100 ± 13.0	108.2 ± 15.9
Iba1	**100 ± 14.7**	**196.6 ± 37.2**[a]	100 ± 21.0	110.9 ± 14.1	100 ± 38.3	93.2 ± 14.6
GFAP	**100 ± 18.1**	**230.3 ± 37.7**[a]	100 ± 33.3	193.8 ± 50.3	100 ± 14.1	133.0 ± 27.3
S100β	100 ± 4.1	85.5 ± 8.7	100 ± 16.0	92.9 ± 14.9	100 ± 3.4	97.9 ± 8.3
4 wk						
NeuN	100 ± 24.2	82.5 ± 20.4	100 ± 30.2	73.0 ± 13.8	100 ± 25.5	126.5 ± 23.8
Iba1	100 ± 13.8	108.1 ± 9.6	100 ± 33.1	190.6 ± 46.5	100 ± 19.5	192.9 ± 37.5
GFAP	**100 ± 7.6**	**185.1 ± 14.4**[a]	100 ± 19.8	149.7 ± 35.7	**100 ± 14.0**	**187.2 ± 30.2**[a]
S100β	**100 ± 6.8**	**121.6 ± 6.0**[a]	100 ± 10.2	110.6 ± 9.1	**100 ± 13.5**	**155.6 ± 18.1**[a]
Synaptic proteins						
6 h						
PSD-95	100 ± 24.7	103.7 ± 32.6	**100 ± 8.7**	**68.7 ± 9.8**[a]	100 ± 25.2	73.7 ± 20.5
NL-1	**100 ± 27.4**	**173.6 ± 15.7**[a]	100 ± 29.2	98.0 ± 32.3	100 ± 44.3	92.1 ± 27.9
N-Cad	100 ± 7.9	109.8 ± 8.3	100 ± 9.3	83.1 ± 16.6	100 ± 58.7	19.3 ± 10.1
Geph	100 ± 10.4	109.8 ± 13.8	100 ± 24.4	75.8 ± 28.6	100 ± 48.4	117.6 ± 43.4
NL-2	100 ± 9.5	110.7 ± 3.8	100 ± 15.3	76.8 ± 15.7	100 ± 10.5	84.7 ± 12.0
NF	100 ± 13.9	134.5 ± 15.5	100 ± 32.6	162.2 ± 45.2	100 ± 19.9	104.8 ± 17.9
Syn I	100 ± 22.9	91.1 ± 19.2	—	—	—	—
Syn II	100 ± 8.3	101.2 ± 7.9	100 ± 12.8	63.1 ± 5.5	—	—
24 h						
PSD-95	100 ± 21.7	107.9 ± 15.1	100 ± 15.9	95.4 ± 14.7	100 ± 10.4	99.8 ± 21.4
NL-1	100 ± 9.0	77.0 ± 21.8	100 ± 6.4	92.2 ± 6.8	100 ± 7.0	97.0 ± 15.4
N-Cad	100 ± 17.5	55.0 ± 11.1	100 ± 7.7	83.3 ± 13.8	100 ± 13.2	86.8 ± 26.5
Geph	100 ± 3.9	99.4 ± 18.9	100 ± 14.4	75.1 ± 17.1	100 ± 7.1	80.0 ± 14.8
NL-2	100 ± 6.9	82.5 ± 10.4	100 ± 16.8	99.5 ± 14.7	100 ± 13.5	61.2 ± 10.4
NF	100 ± 24.9	37.1 ± 9.6	100 ± 18.1	95.3 ± 20.8	100 ± 19.2	53.3 ± 6.2
Syn I	100 ± 5.4	97.5 ± 7.9	100 ± 11.8	97.5 ± 11.4	100 ± 3.0	108.1 ± 4.7
Syn II	100 ± 23.2	142.6 ± 55.6	100 ± 14.4	115.5 ± 9.4	100 ± 9.5	95.7 ± 13.5

(Continues)

TABLE 1 (Continued)

	Ipsilateral HPC		Cortex		Subcortex	
	Ctrl	**NCSE**	**Ctrl**	**NCSE**	**Ctrl**	**NCSE**
1 wk						
PSD-95	100 ± 2.4	79.9 ± 9.1	100 ± 14.6	93.14 ± 8.6	100 ± 10.8	95.5 ± 18.0
NL-1	100 ± 4.2	105.6 ± 3.8	100 ± 10.1	90.7 ± 7.9	100 ± 6.5	89.5 ± 4.6
N-Cad	100 ± 5.2	114.9 ± 7.5	100 ± 5.5	84.4 ± 6.2	**100 ± 4.5**	**84.8 ± 4.2**[a]
Geph	100 ± 1.7	97.2 ± 3.1	100 ± 20.4	80.1 ± 15.4	100 ± 5.6	120.2 ± 19.8
NL-2	**100 ± 4.8**	**86.9 ± 2.1**[a]	100 ± 12.0	98.0 ± 5.7	100 ± 11.1	109 ± 18.7
NF	100 ± 4.0	99.1 ± 2.5	100 ± 12.1	123.9 ± 20.3	100 ± 18.2	91.5 ± 6.7
Syn I	100 ± 7.2	78.8 ± 8.6	100 ± 15.8	106.8 ± 14.7	100 ± 10.5	91.0 ± 15.2
Syn II	**100 ± 7.5**	**59.8 ± 10.0**[a]	100 ± 9.7	80.2 ± 8.5	100 ± 9.3	94.8 ± 14.4
4 wk						
PSD-95	100 ± 16.9	84.9 ± 12.6	100 ± 9.4	100.7 ± 18.7	100 ± 20.3	149.5 ± 51.1
NL-1	100 ± 15.3	68.7 ± 9.6	100 ± 7.8	110.8 ± 6.2	100 ± 30.0	166.2 ± 29.0
N-Cad	100 ± 15.6	119.7 ± 15.1	100 ± 6.8	87.6 ± 6.3	100 ± 15.8	84.5 ± 14.6
Geph	100 ± 6.2	113.7 ± 13.7	100 ± 16.2	104.6 ± 10.0	100 ± 22.9	126.0 ± 32.8
NL-2	100 ± 13.2	120.5 ± 16.8	100 ± 14.4	114.8 ± 22.8	100 ± 9.2	119.9 ± 10.8
NF	100 ± 16.0	103.4 ± 12.8	100 ± 15.2	66.4 ± 9.1	100 ± 30.5	117.0 ± 26.5
Syn I	100 ± 12.9	119.2 ± 16.3	100 ± 6.1	90.3 ± 6.5	100 ± 18.0	130.7 ± 26.5
Syn II	100 ± 9.8	95.5 ± 6.6	**100 ± 9.6**	**123.8 ± 3.2**[a]	100 ± 6.9	112.5 ± 15.1

Data (mean ± standard error of mean) are presented as percentage change relative to Ctrl and normalized to either β-actin (42 kDa) or glyceraldehyde-3-phosphate dehydrogenase (37 kDa). 6 h: Ctrl, n = 6-8; NCSE, n = 7. 24 h: Ctrl, n = 6-8; NCSE, n = 5-6. 1 wk: Ctrl, n = 6; NCSE, n = 4-6. 4 wk: Ctrl, n = 5-12; NCSE, n = 5-16. Bold figures represent significant differences compared to Ctrl.

Ctrl, controls; Geph, gephyrin; GFAP, glial fibrillary acidic protein; HPC, hippocampus; N-Cad, N-cadherin; NCSE, nonconvulsive status epilepticus; NF, neurofascin; NL, neuroligin; PSD, postsynaptic density protein; Syn, synapsin.

[a]$P \leq .05$, unpaired t test.

TABLE 2 Quantification of immunoblots of excitatory and inhibitory synaptic proteins in contralateral hippocampus at 6 hours, 24 hours, and 4 weeks post-NCSE

	6 h		24 h		4 wk	
	Ctrl	**NCSE**	**Ctrl**	**NCSE**	**Ctrl**	**NCSE**
PSD-95	100 ± 6.1	93.4 ± 7.1	100 ± 10.3	101.8 ± 6.0	100 ± 20.6	85.9 ± 14.2
NL-1	100 ± 21.9	92.0 ± 19.5	100 ± 18.3	123.4 ± 17.2	100 ± 11.7	102.5 ± 11.5
N-cadherin	100 ± 12.6	110.1 ± 10.5	100 ± 7.8	96.4 ± 7.9	100 ± 7.0	85.8 ± 6.2
Gephyrin	100 ± 8.6	86.0 ± 6.3	100 ± 17.1	113.1 ± 7.8	100 ± 2.5	103.1 ± 4.2
NL-2	100 ± 10.8	85.2 ± 15.7	100 ± 11.4	99.7 ± 19.3	100 ± 8.5	110.9 ± 101.0
Neurofascin	100 ± 20.1	92.6 ± 17.0	100 ± 28.9	60.2 ± 14.6	100 ± 11.2	128.0 ± 13.8
Synapsin I	100 ± 20.5	101.9 ± 28.8	100 ± 9.5	101.3 ± 13.9	100 ± 6.3	88.4 ± 8.1
Synapsin II	100 ± 30.3	46.2 ± 13.7	100 ± 16.0	97.0 ± 12.7	100 ± 6.7	83.1 ± 12.9

Data (mean ± standard error of mean) are presented as percentage change relative to Ctrl and normalized to either β-actin (42 kDa) or glyceraldehyde-3-phosphate dehydrogenase (37 kDa). 6 h: Ctrl, n = 8; NCSE, n = 7. 24 h: Ctrl, n = 6; NCSE, n = 6. 1 wk: Ctrl, n = 5-6; NCSE, n = 4-6. 4 wk: Ctrl, n = 7-12; NCSE, n = 7-16.

Ctrl, controls; NCSE, nonconvulsive status epilepticus; NL, neuroligin; PSD, postsynaptic density protein.

decrease in NeuN levels in the contralateral HPC following NCSE shown for the entire group was now only significant in rats that developed spontaneous seizures. No decrease was observed in rats with only acute symptomatic seizures; however, there was a trend ($P = .052$; Figure 4A). The lack of changes in cortical and subcortical tissue remained when subdividing the NCSE rats (cortex: Ctrl 100 ± 30.2 vs NCSE+AS 39.1 ± 18.9 vs NCSE+SS 76.5 ± 12.0;

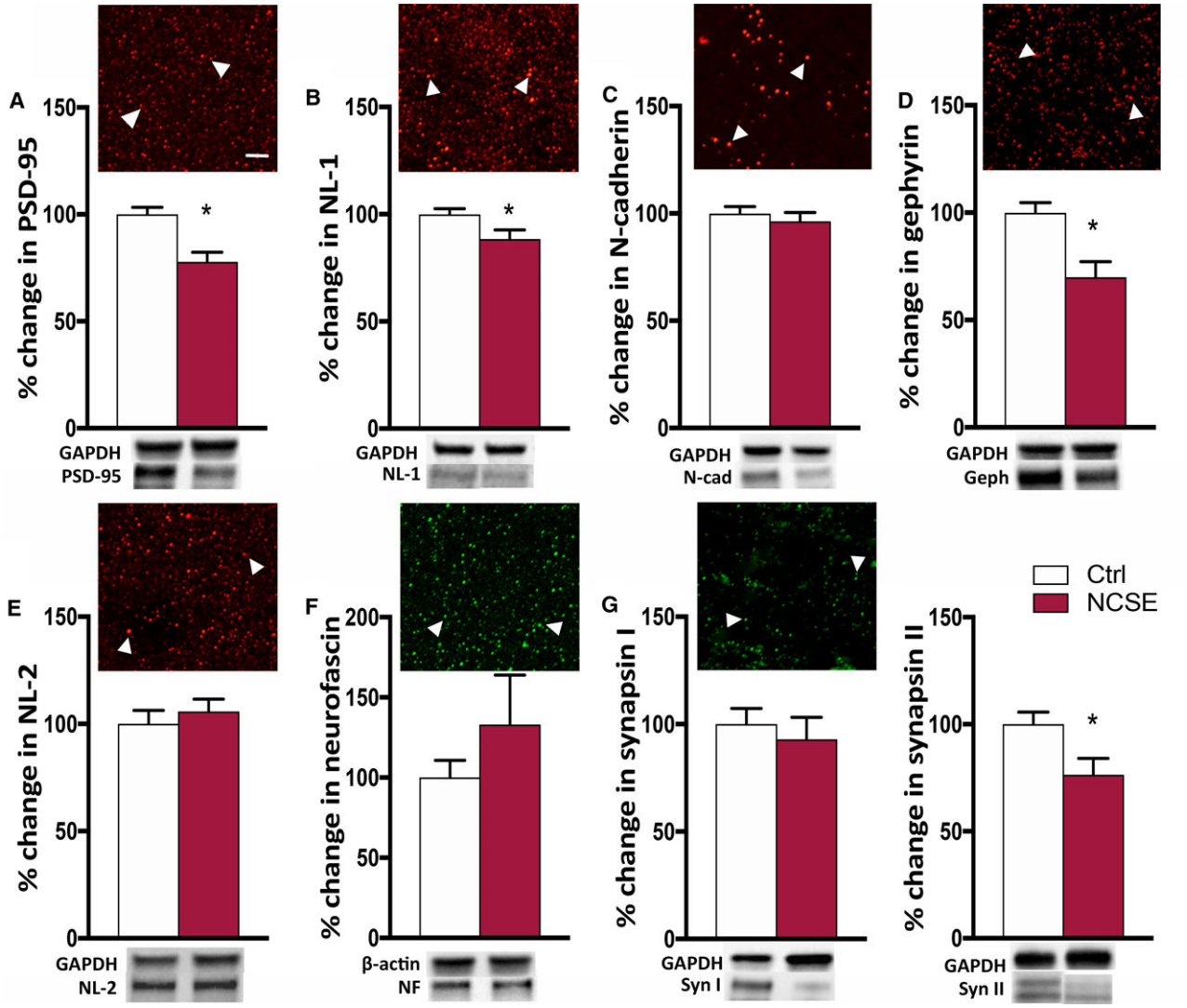

FIGURE 3 Excitatory and inhibitory synaptic protein alterations in the hippocampus 1 week after nonconvulsive status epilepticus (NCSE). Representative immunohistochemical stainings and immunoblots and quantification are shown of postsynaptic density protein 95 (PSD-95; 95 kDa), neuroligin-1 (NL-1; 101 kDa), N-cadherin (120 kDa) gephyrin (95 kDa), neuroligin-2 (NL-2; 93 kDa), neurofascin (NF; 155 kDa), synapsin I (75 kDa), and synapsin II (54 and 74 kDa) in contralateral hippocampus, relative to Ctrl, and normalized to either β-actin (42 kDa) or glyceraldehyde-3-phosphate dehydrogenase (GAPDH; 37 kDa). Data are presented as mean ± standard error of mean; controls (Ctrl), n = 5-6; NCSE, n = 4-6. *$P \leq .05$, unpaired t test. Arrowheads in photomicrographs point toward clusters of synaptic proteins. Scalebar = 5 μm for all parts

subcortex: Ctrl 100 ± 25.5 vs NCSE+AS 86.0 ± 35.0 vs NCSE+SS 146.6).

The increase in Iba1 levels in the contralateral HPC at 4 weeks post-NCSE was evident in both the acute symptomatic and spontaneous seizure group, whereas rats with acute symptomatic seizures contributed the most to the overall increase in GFAP (Figure 4B,C). In contrast to previous measurements of the entire NCSE group, Iba1 levels were now also increased in both cortex and subcortex (cortex: Ctrl 100 ± 33.1 vs NCSE+AS 52.6 ± 24.6 vs NCSE+SS 232 ± 53.6; subcortex Ctrl 100 ± 19.5 vs NCSE+AS 143 ± 65.0 vs NCSE+SS 230 ± 52.4), and GFAP levels were increased in subcortex in rats with NCSE and spontaneous seizures compared to Ctrl (Ctrl 100 ± 14.0 vs NCSE+AS 164.8 ± 73.0 vs NCSE+SS 213.9 ± 37.4). Levels of S100β expression remained unchanged in contralateral HPC (Figure 4D) and cortex, whereas rats with spontaneous seizures exhibited an increase in subcortical tissue (Ctrl 100 ± 13.5 vs NCSE+AS 120.3 ± 24.3 vs NCSE+SS 171.7 ± 26.0). Again, due to possible electrode-induced changes, we detected no alterations in the ipsilateral HPC in NeuN and Iba1 levels, whereas GFAP levels were increased in both groups (Ctrl 100 ± 7.6 vs NCSE+AS 152.2 ± 31.3 vs NCSE+SS 206.9 ± 16.3) and S100β levels were increased in rats with spontaneous seizures compared to Ctrl (Ctrl

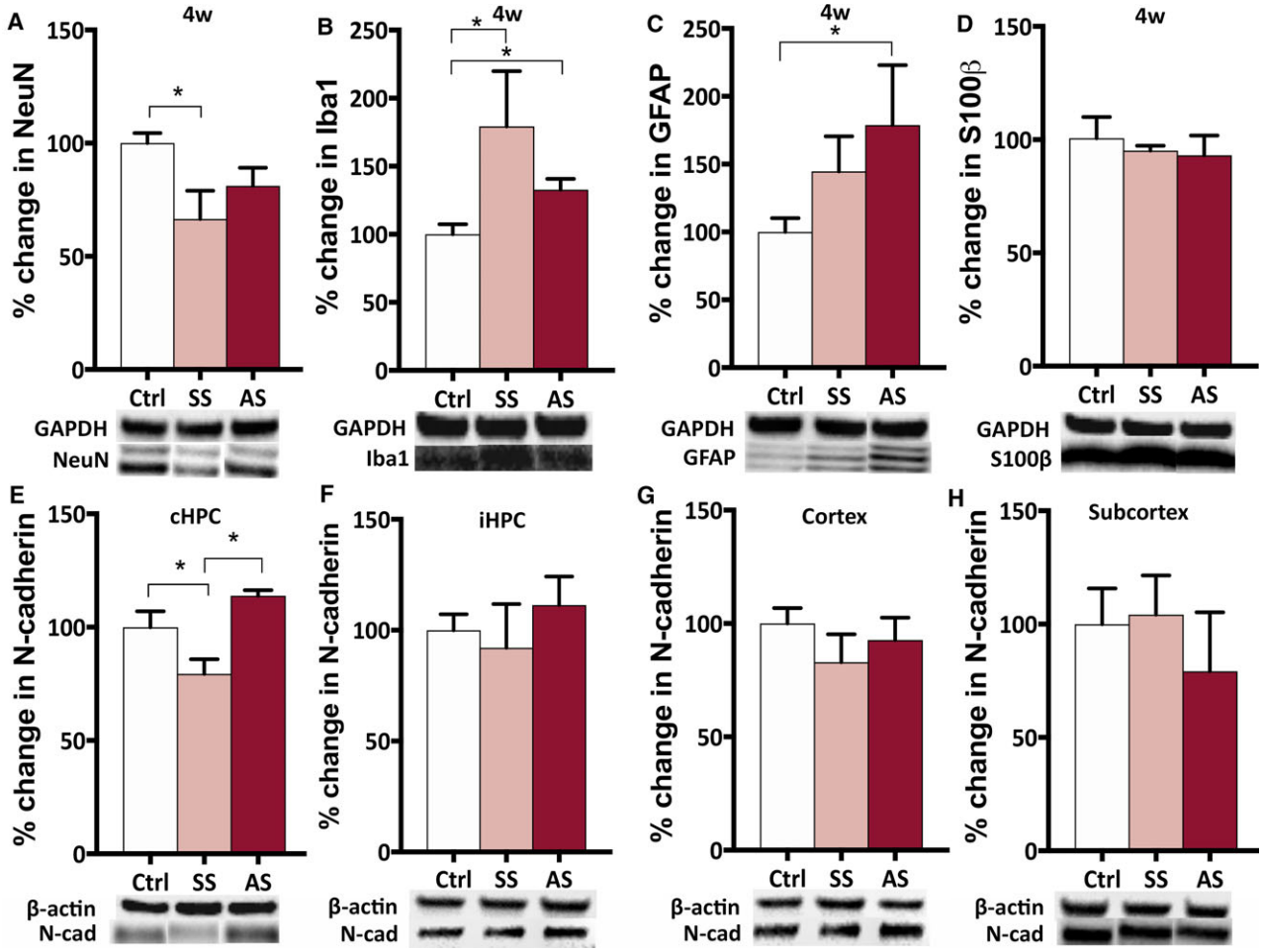

FIGURE 4 Differences in protein levels of nonconvulsive status epilepticus (NCSE) rats developing spontaneous seizures compared to only acute symptomatic seizures. Representative immunoblots and quantification are shown of (A) NeuN (46 kDa), (B) Iba1 (17 kDa), (C) glial fibrillary acidic protein (GFAP; 55 kDa), (D) S100β (11 kDa), and (E) N-cadherin (120 kDa) in contralateral hippocampus (cHPC), (F) N-cadherin in ipsilateral hippocampus (iHPC), (G) N-cadherin in cortex, and (H) N-cadherin in subcortex at 4 weeks after NCSE with either spontaneous seizures (SS) or acute symptomatic seizures (AS) relative to controls (Ctrl), and normalized to either β-actin (42 kDa) or glyceraldehyde-3-phosphate dehydrogenase (GAPDH; 37 kDa). Data are presented as mean ± standard error of mean; Ctrl, n = 7-13; NCSE+SS, n = 3-10; NCSE+AS, n = 3-4. *$P \leq .05$, unpaired *t* test

100 ± 6.8 vs NCSE+AS 120.9 ± 12.0 vs NCSE+SS 121.8 ± 7.2).

3.6 | Decreased N-cadherin levels in NCSE rats with spontaneous compared to acute symptomatic seizures

Rats with spontaneous seizures post-NCSE exhibited decreased levels of N-cadherin in the contralateral HPC compared to rats with only acute symptomatic seizures (Figure 4E). The reduction did not correlate with reduced NeuN levels ($r = -.071$, $P = .91$), suggesting that the N-cadherin reduction was not a result of neuronal death. Also, N-cadherin levels within the NCSE group exhibiting spontaneous seizures did not correlate with the total number or duration of spontaneous seizures per rat during week 2-4 ($r = .56$, $P = .19$ and $r = .49$, $P = .26$, respectively), mean duration of individual spontaneous seizures ($r = -.04$, $P = .94$), or IA load during the same period ($r = .29$, $P = .56$). This may suggest a common underlying course for reduced N-cadherin expression in NCSE rats developing spontaneous seizures, rather than a decrease due to the spontaneous seizures per se. No changes were observed in the ipsilateral HPC, cortical, or subcortical tissue (Figure 4F-H).

4 | DISCUSSION

Apart from being difficult to diagnose in patients, the long-term consequences of NCSE per se have so far been difficult to visualize with standard imaging techniques and

remain unclear. Here we provide evidence for neuronal loss, continuous immune reaction, and alterations in excitatory and inhibitory synaptic proteins in the temporal lobes within 1 month following complex partial NCSE in rats. The histopathology in this experimental model could not be consistently confirmed by DTI of mice with similar NCSE. We noticed that a majority of the animals had no latency period but experienced acute symptomatic seizures during the first week post-NCSE. About 70% of them continued to develop an epileptogenic phase with unprovoked spontaneous focal seizures with or without secondary generalization and IA. NCSE rats that developed spontaneous seizures exhibited an immune reaction that extended outside the epileptic focus and into cortical tissue. In addition, levels of the synaptic adhesion molecule N-cadherin were specifically decreased in the HPC of NCSE rats with concomitant spontaneous seizures, indicating its involvement in the development of epilepsy.

There are few experimental models that mimic NCSE. Low doses of pilocarpine/kainic acid can initiate nonconvulsive seizures/SE,[7,8,30,31] although so far either primarily cortical brain damage or more extensive HPC damage has been reported. Studies on the intrahippocampal kainic acid model describe NCSE in mice for up to 10 hours, followed by a latent phase without acute symptomatic seizures for 2 weeks, before the development of spontaneous seizures. The subsequent pathophysiology shows similarities to HPC sclerosis.[10] The electrical-induced models for epileptic seizures[11] have been utilized extensively for initiating more severe secondary generalized seizures/SE. In the present study, we have instead initiated NCSE with temporal semiology and seldom secondary generalization.[11,17] In clinical practice, many patients present comorbidities, which makes pathology related to the NCSE per se difficult to dissect out. The animals in the electrical model were naive before electrode implantation, meaning no other underlying genetic pathology or acquired factors for epilepsy were present. In addition, no drugs were administered to initiate the seizures. Neither the amount of acute symptomatic seizures nor the load of IA predicted the risk of developing spontaneous seizures, which underscores the importance of exploring new biomarkers for epileptogenesis. Almost all of the NCSE rats developed acute symptomatic seizures, but 30% did not continue with spontaneous seizures within 4 weeks post-NCSE. It is possible that some rats would have developed seizures at later time points, but the data still support previous clinical studies suggesting that acute symptomatic seizures cannot be used as a strong predictor of epileptogenesis even if they are associated with an increased risk.[19,20,32,33]

We conclude from the current study that ex vivo DTI at 9.4 T did not provide convincing results for detection of microstructural changes within the epileptic focus following experimental NCSE without extensive HPC sclerosis. Power calculations ($P = .80$) suggest an additional sample size of >10 mice per group to detect differences in FA. However, the presented 9.4-T DTI FA maps were included primarily to shed light on the problem that, on an individual level, cellular alterations after NCSE are variable and sometimes undetectable. Given that the current first-line tool for investigating epileptic insults is 1.5–3-T MRI scanners and that few studies have been able to localize long-lasting changes in the brain following NCSE,[5,6] future studies may have to combine more advanced MRI methods with other imaging techniques, such as new positron emission tomography isotopes, to increase the sensitivity for seizure-induced changes.

With only minor exceptions, the increase in glial activation and neuronal loss at 1 and 4 weeks post-NCSE was most prominent in the epileptic focus, particularly in the CA1 region of the HPC. Changes in subgroups of cortical and subcortical neurons may be missed due to sensitivity limits of the Western blot analyses. Nonetheless, within the epileptic focus small changes in protein levels related to inhibitory neurons were observed, which strengthens previous immunohistochemical findings.[17] Early neurodegeneration post-NCSE within CA regions further supports the finding of neuronal cell loss. In addition, the Iba1 and GFAP levels peaked at 1 week, concurrently with a previously described increase in cells expressing the glial marker ED1.[18] Whether the inflammatory profile may exhibit proinflammatory or anti-inflammatory properties is not revealed by levels of Iba1, GFAP, or S100β. A heterogenous immune profile has also been described for hippocampal, cortical, and cerebellar areas following a similar electrical SE model of nonconvulsive plus convulsive seizures.[26] The present finding with an altered morphology of microglia within the HPC merely suggests a more activated profile. Preliminary data from our group indicate a transient early HPC increase and systemic release of cytokines and chemokines already 6 hours post-NCSE (Avdic et al, unpublished observations). Additionally, in NCSE rats that developed spontaneous seizures, a cortical glial reaction could indicate larger network involvement, which is supported by clinical functional MRI studies of temporal lobe epilepsy.[34]

The glial reaction was accompanied by a transient acute rearrangement of excitatory and inhibitory synaptic properties. The overall decrease in pivotal synaptic proteins may either propagate the pathophysiology and increase the susceptibility for having or initiating spontaneous seizures or merely reflect a dampening reaction to a prolonged abnormal synchronized activity as that of NCSE. Irrespectively, the synaptic reaction may be involved in the development of epilepsy. We have previously documented alterations in the same synaptic proteins

prior to the occurrence of provoked generalized seizures in genetically modified mice depleted of synapsin II,[21] and gephyrin levels are reduced after pilocarpine-induced convulsive SE.[35] Several of these synaptic proteins can also be disrupted in patients with epilepsy.[36–39] At 4 weeks post-NCSE, only levels of the excitatory adhesion molecule N-cadherin were reduced in epileptic rats, compared to rats with acute symptomatic seizures. Selective loss of N-cadherin by conditional ablation of excitatory synapses has been shown to increase the density of inhibitory synaptic proteins and decrease PSD-95, suggesting a seizure-promoting effect for N-cadherin.[40]

The functional consequences for cognition and other behavioral tasks post-NCSE are not clear. Although previous studies have reported altered social interaction and motor deficits in rats following NCSE induced by low-dose pilocarpine,[31] the long-term pathology detected in our model is not associated with changes in spatial working memory assessed with Y-maze, forced swim test, or open field and social interaction test for signs of depression, anxiety or impaired social behavioral traits, respectively (Avdic et al, unpublished observations).

5 | CONCLUSION

Our report provides evidence for an experimental rodent model of NCSE with several similarities to clinical practice in terms of periictal and interictal EEG patterns, semiology, and development of acute symptomatic and spontaneous seizures. It describes the ignition of long-lasting NCSE-induced pathophysiological changes in the brain, including neuronal loss, immune reaction, and synaptic rearrangements, which are not readily detected with high-resolution DTI imaging. The model is also promising for future clinical predictions of biomarkers and therapeutic strategies for epilepsy.

ACKNOWLEDGMENTS

The research leading to these results has received funding from the European Union's Seventh Framework Program (FP7/2007-2013) under grant agreement 602102 (EPITARGET), Swedish Research Council, Crafoord Foundation, ALF Grant for funding for medical training and research, and Academy of Finland (275453). We thank biomedical analysts Susanne Jonsson for technical support.

DISCLOSURE

None of the authors has any conflict of interest to disclose. We confirm that we have read the Journal's position on issues involved in ethical publication and affirm that this report is consistent with those guidelines.

REFERENCES

1. Holtkamp M, Meierkord H. Nonconvulsive status epilepticus: a diagnostic and therapeutic challenge in the intensive care setting. Ther Adv Neurol Disord. 2011;4:169–81.
2. Trinka E, Cock H, Hesdorffer D, et al. A definition and classification of status epilepticus—report of the ILAE Task Force on Classification of Status Epilepticus. Epilepsia. 2015;56:1515–23.
3. Walker MC. Treatment of nonconvulsive status epilepticus. Int Rev Neurobiol. 2007;81:287–97.
4. Williamson PD, Spencer DD, Spencer SS, et al. Complex partial seizures of frontal lobe origin. Ann Neurol. 1985;18:497–504.
5. Jabeen SA, Cherukuri P, Mridula R, et al. A prospective study of diffusion weighted magnetic resonance imaging abnormalities in patients with cluster of seizures and status epilepticus. Clin Neurol Neurosurg. 2017;155:70–4.
6. Szabo K, Poepel A, Pohlmann-Eden B, et al. Diffusion-weighted and perfusion MRI demonstrates parenchymal changes in complex partial status epilepticus. Brain. 2005;128:1369–76.
7. Ben-Ari Y. Limbic seizure and brain damage produced by kainic acid: mechanisms and relevance to human temporal lobe epilepsy. Neuroscience. 1985;14:375–403.
8. Krsek P, Mikulecka A, Druga R, et al. An animal model of nonconvulsive status epilepticus: a contribution to clinical controversies. Epilepsia. 2001;42:171–80.
9. Loscher W. Animal models of epilepsy for the development of antiepileptogenic and disease-modifying drugs. A comparison of the pharmacology of kindling and post-status epilepticus models of temporal lobe epilepsy. Epilepsy Res. 2002;50:105–23.
10. Riban V, Bouilleret V, Pham-Le BT, et al. Evolution of hippocampal epileptic activity during the development of hippocampal sclerosis in a mouse model of temporal lobe epilepsy. Neuroscience. 2002;112:101–11.
11. Lothman EW, Bertram EH, Bekenstein JW, et al. Self-sustaining limbic status epilepticus induced by 'continuous' hippocampal stimulation: electrographic and behavioral characteristics. Epilepsy Res. 1989;3:107–19.
12. Chih B, Engelman H, Scheiffele P. Control of excitatory and inhibitory synapse formation by neuroligins. Science. 2005;307:1324–8.
13. Dalva MB, McClelland AC, Kayser MS. Cell adhesion molecules: signalling functions at the synapse. Nat Rev Neurosci. 2007;8:206–20.
14. Arikkath J, Reichardt LF. Cadherins and catenins at synapses: roles in synaptogenesis and synaptic plasticity. Trends Neurosci. 2008;31:487–94.
15. Ben-Ari Y. Cell death and synaptic reorganizations produced by seizures. Epilepsia. 2001;42(suppl 3):5–7.
16. Farber K, Kettenmann H. Physiology of microglial cells. Brain Res Brain Res Rev. 2005;48:133–43.
17. Mohapel P, Ekdahl CT, Lindvall O. Status epilepticus severity influences the long-term outcome of neurogenesis in the adult dentate gyrus. Neurobiol Dis. 2004;15:196–205.
18. Ekdahl CT, Claasen JH, Bonde S, et al. Inflammation is detrimental for neurogenesis in adult brain. Proc Natl Acad Sci U S A. 2003;100:13632–7.

19. Beghi E, Carpio A, Forsgren L, et al. Recommendation for a definition of acute symptomatic seizure. Epilepsia. 2010;51:671–5.
20. Beleza P. Acute symptomatic seizures: a clinically oriented review. Neurologist. 2012;18:109–19.
21. Chugh D, Ali I, Bakochi A, et al. Alterations in brain inflammation, synaptic proteins, and adult hippocampal neurogenesis during epileptogenesis in mice lacking synapsin2. PLoS One. 2015;10:e0132366.
22. Ali I, Chugh D, Ekdahl CT. Role of fractalkine-CX3CR1 pathway in seizure-induced microglial activation, neurodegeneration, and neuroblast production in the adult rat brain. Neurobiol Dis. 2015;74:194–203.
23. Husain AM, Mebust KA, Radtke RA. Generalized periodic epileptiform discharges: etiologies, relationship to status epilepticus, and prognosis. J Clin Neurophysiol. 1999;16:51–8.
24. Kaplan PW. Prognosis in nonconvulsive status epilepticus. Epileptic Disord. 2000;2:185–93.
25. Sierra A, Laitinen T, Lehtimaki K, et al. Diffusion tensor MRI with tract-based spatial statistics and histology reveals undiscovered lesioned areas in kainate model of epilepsy in rat. Brain Struct Funct. 2011;216:123–35.
26. Gorter JA, van Vliet EA, Aronica E, et al. Potential new antiepileptogenic targets indicated by microarray analysis in a rat model for temporal lobe epilepsy. J Neurosci. 2006;26:11083–110.
27. McBain CJ, Fisahn A. Interneurons unbound. Nat Rev Neurosci. 2001;2:11–23.
28. Chia PH, Li P, Shen K. Cell biology in neuroscience: cellular and molecular mechanisms underlying presynapse formation. J Cell Biol. 2013;203:11–22.
29. Song JY, Ichtchenko K, Sudhof TC, et al. Neuroligin 1 is a postsynaptic cell-adhesion molecule of excitatory synapses. Proc Natl Acad Sci U S A. 1999;96:1100–5.
30. Benson MJ, Manzanero S, Borges K. Complex alterations in microglial M1/M2 markers during the development of epilepsy in two mouse models. Epilepsia. 2015;56:895–905.
31. Krsek P, Mikulecka A, Druga R, et al. Long-term behavioral and morphological consequences of nonconvulsive status epilepticus in rats. Epilepsy Behav. 2004;5:180–91.
32. Hesdorffer DC, Benn EK, Cascino GD, et al. Is a first acute symptomatic seizure epilepsy? Mortality and risk for recurrent seizure. Epilepsia. 2009;50:1102–8.
33. Hesdorffer DC, Logroscino G, Cascino G, et al. Risk of unprovoked seizure after acute symptomatic seizure: effect of status epilepticus. Ann Neurol. 1998;44:908–12.
34. Caciagli L, Bernhardt BC, Hong SJ, et al. Functional network alterations and their structural substrate in drug-resistant epilepsy. Front Neurosci. 2014;8:411.
35. Gonzalez MI, Cruz Del Angel Y, Brooks-Kayal A. Down-regulation of gephyrin and GABAA receptor subunits during epileptogenesis in the CA1 region of hippocampus. Epilepsia. 2013;54:616–24.
36. Lionel AC, Vaags AK, Sato D, et al. Rare exonic deletions implicate the synaptic organizer Gephyrin (GPHN) in risk for autism, schizophrenia and seizures. Hum Mol Genet. 2013;22:2055–66.
37. Millson A, Lagrave D, Willis MJ, et al. Chromosomal loss of 3q26.3-3q26.32, involving a partial neuroligin 1 deletion, identified by genomic microarray in a child with microcephaly, seizure disorder, and severe intellectual disability. Am J Med Genet A. 2012;158A:159–65.
38. Shimojima K, Sugawara M, Shichiji M, et al. Loss-of-function mutation of collybistin is responsible for X-linked mental retardation associated with epilepsy. J Hum Genet. 2011;56:561–5.
39. Ying Z, Bingaman W, Najm IM. Increased numbers of coassembled PSD-95 to NMDA-receptor subunits NR2B and NR1 in human epileptic cortical dysplasia. Epilepsia. 2004;45:314–21.
40. Nikitczuk JS, Patil SB, Matikainen-Ankney BA, et al. N-cadherin regulates molecular organization of excitatory and inhibitory synaptic circuits in adult hippocampus in vivo. Hippocampus. 2014;24:943–62.

SUPPORTING INFORMATION

Additional Supporting Information may be found online in the supporting information tab for this article.

How to cite this article: Avdic U, Ahl M, Chugh D, et al. Nonconvulsive status epilepticus in rats leads to brain pathology. *Epilepsia*. 2018;59:945–958. https://doi.org/10.1111/epi.14070